Soria 6-7-8
Octubre
2014

II Congreso Iberoamericano

Microrredes con Generación Distribuida de Renovables

(Aplicaciones prácticas
de integración de
energías renovables
a Sitios de la UNESCO)

lunes 6

8:30h
Recepción y registro.

9:30h
Bienvenida del Alcalde de la ciudad de Soria y de la Subdelegada del Gobierno de la Provincia de Soria.

Apertura del II Congreso Iberoamericano sobre Microrredes con Generación Distribuida de Renovables.

Sesión 1

ENERGÍAS RENOVABLES Y REDUCCIÓN DE EMISIONES. APLICACIONES PRÁCTICAS DE INTEGRACIÓN A SITIOS DE LA UNESCO
Moderador: **Miguel Latorre** CEDER-CIEMAT (Centro de Desarrollo de Energías Renovables).

10:00h
SISTEMA DE GESTIÓN DE ENERGÍA PARA MICRORREDES
CEIT (Centro de estudios e investigaciones técnicas de Guipúzcoa).

10:20h
MEJORA DE LA CALIDAD DE VIDA CON EL USO DE FUENTES RENOVABLES DE ENERGIA EN LA COMUNIDAD LAS POZAS, GRAN HUMEDAL DEL NORTE (SITIO RAMSAR 1125), CIEGO DE ÁVILA, CUBA. UN ANTES Y UN DESPUÉS.
CUBASOLAR (Sociedad Cubana para la Promoción de las Fuentes Renovables de Energía), Ministerio de Ciencia, Tecnología y Medio Ambiente, Cuba.

10:40h
ENERGÍAS RENOVABLES Y REDUCCIÓN DE EMISIONES. ENERGÍA EÓLICA
CEETA (Center of Energy and Environmental Technical Studies), Cuba.

11:00h
Café

Sesión 2

REDES INTELIGENTES, MEDIDA INTELIGENTE, MICRORREDES
Moderador: **Luis Cano** CEDER-CIEMAT (Centro de Desarrollo de Energías Renovables)

12:00h
MICROGENERACIÓN/ MINIGENERACIÓN RENOVABLE DISTRIBUIDA Y SU CONTROL
MIRED-CON CEDER-CIEMAT (Centro de Desarrollo de Energías Renovables), ZIV Group Company, Universidad Complutense de Madrid.

12:20h
ARQUITECTURA DE LOS SISTEMAS DE CONTROL Y COMUNICACIONES EN MICRORREDES ELÉCTRICAS INTELIGENTES
Universidad Politécnica de Cataluña.

12:40h
SMART ENERGY INTEGRATION LAB (SEIL): TECNOLOGÍA PHIL APLICADA AL ESTUDIO DE LAS MICRORREDES
Instituto IMDEA Energía.

13:00h
DISEÑO OPTIMIZADO DE UNA ISLA ENERGÉTICA MEDIANTE TÉCNICAS DE BARRIDO PARAMÉTRICOPARAMÉTRICO
CETA-CIEMAT (Centro Extremeño de Tecnologías Avanzadas).

13:20h
PREDICCIÓN DE DEMANDA ELÉCTRICA: ANTECEDENTES, ACTUALIDAD Y TENDENCIAS DE FUTURO
INTEC (Instituto tecnológico de Santo Domingo), República Dominicana, CEDER-CIEMAT (Centro de Desarrollo de Energías Renovables).

13:40h
IMPLEMENTACIÓN DE SISTEMAS DE TELEMETRÍA EN EMPRESA DISTRIBUIDORA DE ENERGÍA ELÉCTRICA SAESA
Empresa de Distribución Eléctrica SAESA, UDEC (Universidad de Concepción), Chile.

14:30h
Comida

19:30h
Conferencia
"ENERGÍAS RENOVABLES Y RESERVAS DE LA BIOSFERA"
(Salón de plenos del Ayuntamiento de Soria)
Cipriano Marín
Responsable de la iniciativa RENFORUS-UNESCO (Renewable Energy Futures for UNESCO Sites).

martes 7

Sesión 3

ENERGÍAS RENOVABLES Y REDUCCIÓN DE EMISIONES. APLICACIONES PRÁCTICAS DE INTEGRACIÓN A SITIOS DE LA UNESCO
Moderador: **Miguel Latorre**
CEDER-CIEMAT (Centro de Desarrollo de Energías Renovables)

09:30h
NUEVO MODELO DE DISTRIBUCIÓN DE CORRIENTE CONTINUA EN BAJA TENSIÓN EN SMART BUILDINGS
CIEMAT (Centro de Desarrollo de Energías Renovables), Universidad de Zaragoza, Universidad Politécnica de Madrid

09:50h
HIBRIDACIÓN CON EERR EN UNA INDUSTRIA – VENEZUELA
Zigor

10:10h
ELECTRIFICACIÓN SUSTENTABLE DE LA ISLA HOLBOX UN ESTUDIO DE CASO
Instituto de Investigaciones Eléctricas, México.

10:30h
MODERGIS, EN LA INTEGRACIÓN DE ENERGÍAS RENOVABLES Y SOSTENIBLES, EN ZONAS SENSIBLES Y AUTOSUFICIENTES
Universidad Nacional de Colombia, CIEMAT (Centro de Investigaciones Energéticas Medioambientales y Tecnológicas).

10:50h
EMPLEO DE FUENTES RENOVABLES DE ENERGÍA EN CUBA
CUBAENERGÍA, Cuba

11:30h
Café

Sesión 4

REDES INTELIGENTES, MEDIDA INTELIGENTE, MICRORREDES
Moderador: Luis Hernández, CEDER-CIEMAT (Centro de Desarrollo de Energías Renovables)

12:00h
PROYECTO OVI-RED: OPERADOR VIRTUAL DE MICRORREDES
Instituto Tecnológico de la Energía.

12:20h
CARACTERIZACIÓN MECÁNICA Y ELÉCTRICA DE UN SISTEMA DE ALMACENAMIENTO RÁPIDO PARA SU OPERACIÓN EN UNA MICRORRED
CIEMAT (Centro de Investigaciones Energéticas Medioambientales y Tecnológicas).

12:40h
CONCEPTUALIZACIÓN Y SIMULACIÓN DE ALGORITMO DE MANEJO ENERGÉTICO PARA UN SISTEMA BESS INTEGRADO A UNA MICRORRED PV
UDEC (Universidad de Concepción), Chile.

13:00h
ESCENARIO ENERGÉTICO EN CENTROAMÉRICA: OPORTUNIDADES Y DESAFÍOS PARA LA MICROGENERACIÓN
The Abdus Salam International Centre for Theoretical Physics (Italy), Instituto Tecnológico de Costa Rica (Costa Rica).

13:20h
IMPROVING THE STORAGE CAPABILITY OF A MICROGRID WITH A VEHICLE-TO-GRID INTERFACE
Polytechnic Institute of Bragança (Portugal).

14:00h
MICRORRED DE LABORATORIO PARA LA EMULACIÓN DE RECURSOS ENERGÉTICOS DISTRIBUIDOS CITCEA-UPC
(Centre d'Innovació Tecnològica en Convertidors Estàtics i Accionaments)

19:00h
Visita cultural por Soria.

miércoles 8

8:30h
Visita a parajes naturales del municipio de Soria.

octubre 2014
Palacio de la Audiencia
Para información adicional:
www.microrredesinteligentes.com

CEDER-CIEMAT
+34 975 28 10 13
info@microrredesinteligentes.com

IMPROVING THE STORAGE CAPABILITY OF A MICROGRID WITH A VEHICLE-TO-GRID INTERFACE

Thematic topic 1: Smart grids / Smart Measurement / Microgrids

Vicente Leite[1], Ângela Ferreira[2] and José Batista[3]

[1] Polytechnic Institute of Bragança, School of Technology and Management, Campus de Santa Apolónia, Apartado 1134, 5301-857 Bragança, Portugal, avtl@ipb.pt

[2] Polytechnic Institute of Bragança, School of Technology and Management, Campus de Santa Apolónia, Apartado 1134, 5301-857 Bragança, Portugal, apf@ipb.pt

[3] Polytechnic Institute of Bragança, School of Technology and Management, Campus de Santa Apolónia, Apartado 1134, 5301-857 Bragança, Portugal, jbatista@ipb.pt

ABSTRACT

In the emergent deployment of microgrids, storage systems play an important role providing ancillary services, such as backup power and reactive power support. This concept becomes crucial in the context of microgrids with a high penetration of renewable energy resources, where storage systems may be used to smooth the intermittency and variability of most of them. Plug-in electric vehicles provide an enormous distributed storage capability, which favours the technical and economical exploitation of such systems. This paper presents a comprehensive implementation and control of a bidirectional power converter for Vehicle-to-Grid integration, based on a bidirectional DC/DC converter followed by a full bridge DC/AC converter. The evaluation of the adopted topology and its control is performed through MATLAB/Simulink simulation.

Keywords: Batteries, Distributed generation, Grid-to-Vehicle, Microgrids, Vehicle-to-Grid.

1. INTRODUCTION

World primary energy demand is projected to increase by 1,2% per year, on average, from now until 2035. Electricity demand is projected to grow by a higher rate, 2,2% per year, considering it is expected that applications, formerly based on chemical energy, will be based on electrical energy in the following decades (IEA, 2012). Besides, the need for dependency reduction on imported fossil fuels has become crucial due to long-lasting instability in many fossil fuel-producing countries which increases the price of energy and reinforces the need to find alternatives. Furthermore, a dramatic reduction of carbon dioxide emissions (CO_2), addressed by various organizations and strategy maps, can only be achieved by reducing the usage of fossil fuels. CO_2 emissions are, in large scale, determined by the level of energy-intensive activity, in particular related to power generation, including heat production, basic materials industry (iron and steel manufacturing) and road transport (Olivier, *et al.*, 2013).

In order to cope with this scenario, changes in energy efficiency are required along with a shift in fuel mix, from fossil fuels to renewable energies, foreseeing a sustainable and environmentally friendlier development. At the present, there is a wide-spread integration of distributed renewable energy sources. By the end of 2012, the power capacity from renewable energy supplied an estimated 22% of global electricity (UNEP, 2013). The penetration of renewable energy sources (RES) tends to grow, since the competitiveness of solar and wind

power is improving considerably (Olivier, *et al.*, 2013). In this context, distribution energy systems are more efficiently exploited into a microgrid concept, *i.e.*, a local network integrating renewable and/or non-renewable distributed energy resources (DER), energy storage devices and loads, guaranteeing security and reliability parameters. Microgrids may operate as standalone systems or connected to the utility grid, contributing to electrification of remote areas and allowing consumers to produce energy to their own requirements whilst reducing the actual stress of power transmission systems (Guerrero, *et al.*, 2013a; Guerrero, *et al.*, 2013b). Microgrids have no spinning reserves like classical utility grid and most microsources have a delayed response when implementing secondary voltage and frequency response. From this point of view, intermediate storage units and micro sources with built-in battery banks are therefore expected to offer the advantages like spinning reserves.

Another feature in the energy sector paradigm is the deployment of electric propulsion systems, representing one of the most promising pathways to address future energy requirements. Plug-in electric vehicles (PEV), hybrid and fuel-cells vehicles are replacing internal combustion engine (ICE) vehicles, with similar driven performance, better efficiency, passenger comfort and safety (Zhang, Cooke, 2010; Zandi, *et al.*, 2011). According to 2012 data, electric vehicle deployment has a distinct geographic distribution: United States has the largest share of hybrid electric vehicles sales (70%), Japan holds the second position (12%) and Netherlands the third position (8%); regarding PEV sales, Japan holds the largest share (28%) followed by the United States (26%) and China (16%) (EVI, IEA, 2013). Battery costs are coming down, more than halving in four years, which together with consumer education and national policy initiatives, contribute to mass-market deployment in future years (EVI, IEA, 2013).

PEV have an important advantage when compared with ICE vehicles and also self-contained hybrid electric vehicles: a distributed energy storage capacity which can be connected to the grid providing ancillary services such as backup active power, acting as a manageable load and discharging energy back to the grid when necessary, reactive power support and peak-shaving. This potential is especially important under the context of microgrids with a high penetration of RES: the additional storage capability may be used to smooth the intermittency and variability of most RES and provide a balance in system cost for grid-integrated storage systems. In fact, energy storage may enhance the exploitation of RES, improving the payback period and also contribute to the frequency and voltage stability strategies of the microgrid.

To do so, battery chargers should be deployed, allowing a bidirectional power flow, by acting as a manageable backup power device and discharging energy back to the grid when necessary, in a grid-to-vehicle (G2V) and vehicle-to-grid (V2G) concept, respectively, engendering the G2V/G2V interface technologies (Ferdowsi, 2007; Saber, Venayagamoorthy, 2009, 2011; Zhang, Cooke, 2010; Yilmaz, Krein, 2013).

This paper presents a bidirectional power converter topology and the implemented control strategy, for the integration of the battery of an electric vehicle in a small microgrid. The power converter topology was introduced in (Leite, *et al.*, 2013a) and the control strategy has been improved in (Leite, *et al.*, 2014). In this work, the reactive power compensation is implemented through the power converter by means of the control of the quadrature component of the grid current, under a vector control scheme, which provides a continuously variable reactive power injection or absorption to the electrical grid, upon its lagging or leading power factor, respectively.

The remaining contents of this paper are organized as follows: main infrastructures of the IPB microgrid are briefly described in Section 2 and the bidirectional power topology for G2V/V2G integration, as well as the control strategy are described in Section 3; section 4 presents the implemented simulation procedure using MATLAB/Simulink, in order to validate the proposed power converter topology and control schemes; finally, in Section 5, there are drawn the main conclusions of the paper.

2. IPB MICROGRID INFRASTRUCTURES

The IPB microgrid has been developed as a research platform and also for demonstration purposes in the context of an university campus, as part of a wider project named VERCampus – Live Campus of Renewable Energies – which integrates a set of technologies, infrastructures and initiatives which have been carried out in

the university Campus of the Polytechnic Institute of Bragança (IPB). The main purpose of this project is to promote DER with integration of renewable energies technologies, for IPB students, stakeholders and all community in general.

The microgrid under consideration is schematically presented in Figure 1 and has been developed for isolated and self-sustainable systems up to a rated power of 5 kW integrating RES with the purpose of being a demonstration platform in terms of technology transfer and applied research (Leite, *et al.*, 2012a). It uses the bidirectional inverter Sunny Island 5048, from SMA, which is the core equipment responsible for the management of the energy flow, and incorporates the following DER: a small 1,4 kWp wind turbine; a solar tracker with a 3 kWp photovoltaic (PV) string; a 2 kWp PV string installed on the roof of the laboratory; a 5 kW back-up diesel generator, powered by a mix with 40% of biodiesel produced from wasted oils in the biofuels laboratory and a 200 Ah battery bank.

A pico run-of-river hydropower plant with 1 kWp (Leite, *et al.*, 2012b) and a 1,34 Wp photovoltaic glass facade are also under development and will be integrated into the microgrid in the foreseeable future.

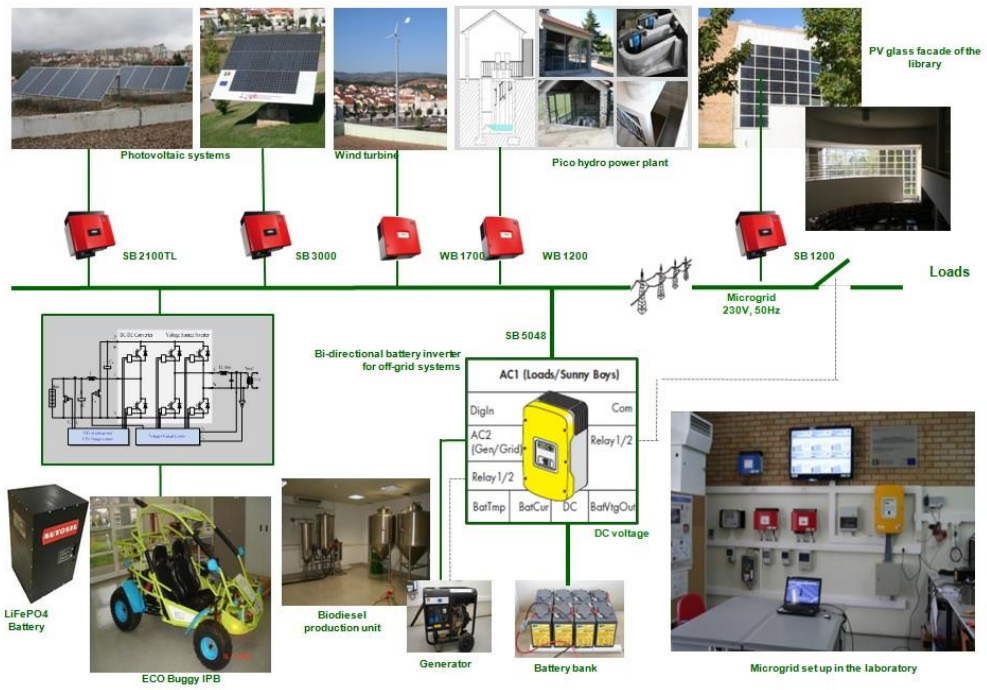

Figure 1.- Illustration of the implemented microgrid.

Another interesting infrastructure is the electric vehicle IPB ECO Buggy, shown in Figure 2, whose battery is to be integrated into the microgrid as an additional energy storage element, including several ancillary services, by using a suitable power converter topology and control schemes.

Figure 2.- The IPB ECO Buggy.

The IPB ECO Buggy is a light electric vehicle using state-of-the-art technology with respect to the electric propulsion system (Leite, *et al.*, 2013b). The chosen electric motor is an axial flux permanent magnet synchronous machine (PMSM), due to its high efficiency, torque and power density. A lithium iron phosphate

battery, with a capacity of 70 Ah and rated voltage of 96 V, was chosen for the IPB ECO Buggy due to its advantages (Leite, *et al.*, 2013b, 2014). In fact, lithium iron phosphate (LiFePO4) has been investigated intensively (Hua, Syue, 2010; Zaghib, *et al.*, 2004) as a potential cathode material for rechargeable lithium ion batteries due to the low cost of raw materials, long life cycle and superior safety characteristics (Hua, Syue, 2010; Tingting, *et al.*, 2011).

3. BIDIRECTIONAL POWER CONVERTER TOPOLOGY FOR V2G/G2V INTEGRATION

The converter topology is based on a bidirectional DC/DC converter followed by a full bridge DC/AC converter. The first works as a buck converter for charging the battery (G2V mode) and as a boost converter for injecting current into the grid (V2G mode). The second is a vector controlled single-phase voltage source inverter (VSI).

The converter topology and the basic control schemes are shown in Figure 3. The shadowed area in Figure 3 (a) represents an integrated power module from Powerex that is being used in the laboratory platform to implement the V2G/G2V interface. In this case the first leg is used to implement the DC/DC converter and the second and third legs are used as a single-phase VSI.

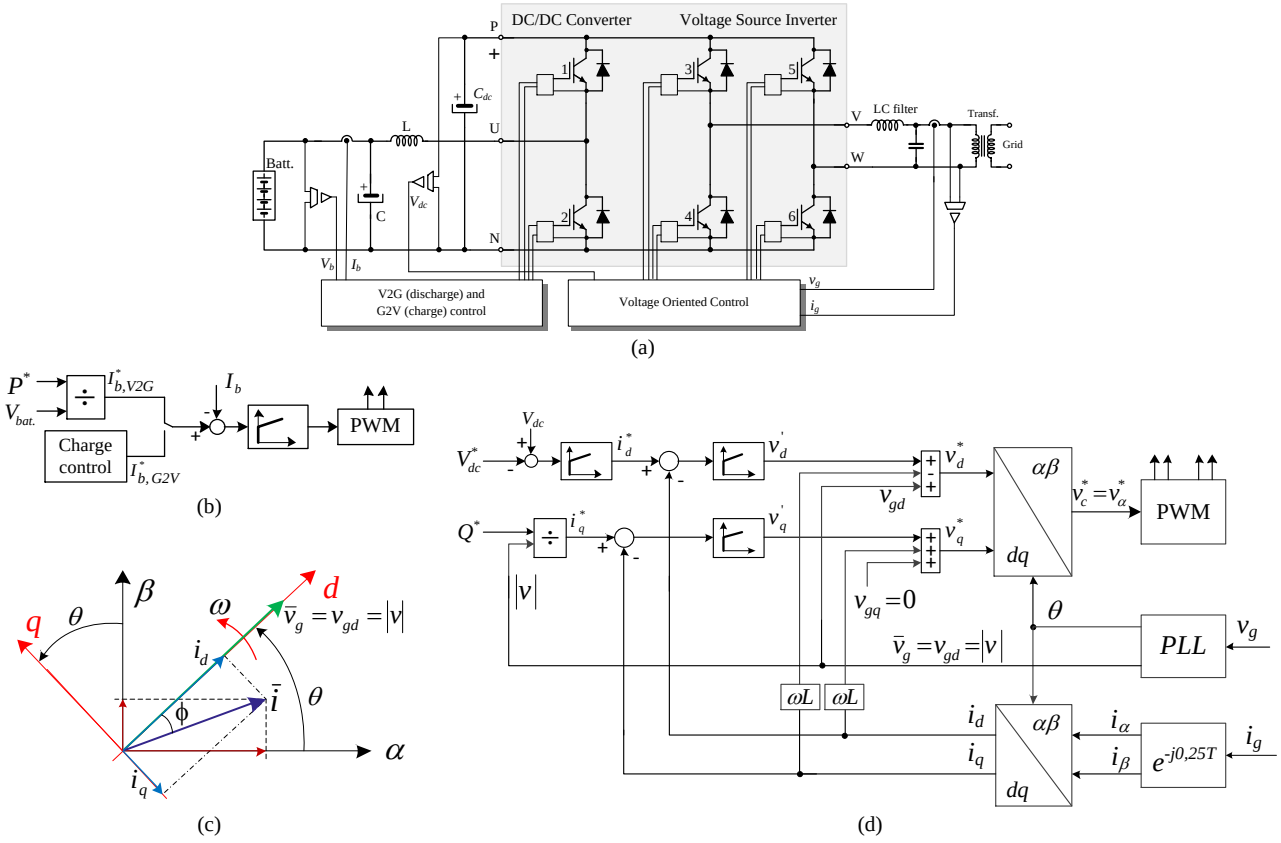

Figure 3.- Converter topology (a) and control schemes: (b) V2G (discharge) and G2V (charge) control; (c) Voltage Oriented Control of the VSI; (d) VOC scheme.

3.1. Control of the DC/DC converter

For the control of the DC/DC converter in V2G mode (discharging mode) the IGBT 1 is always turned OFF and the IGBT 2 is turned ON and OFF at the switching frequency. The IGBT 2, the inductor L and the diode 1 (of IGBT 1) operate as a boost converter. The reference current, $I^*_{b,V2G}$, is set according to the power to be injected into the grid and the maximum admissible depth of discharge. On the other hand, to control the

DC/DC converter in G2V mode (charging mode), the IGBT 2 is always turned OFF and the IGBT 1 is turned ON and OFF at the switching frequency. The IGBT 1, the inductor *L*, the capacitor *C* and the diode 2 (of IGBT 2) operate as a buck converter. In this case, the reference current, $I^*_{b,G2V}$, and the reference battery voltage, are set according to a three-stage charge curve defined by the battery manufacturer.A PI current controller compares the reference current with the measured one, I_b, and generates the control signal for pulse generation (Figure 3 (b)).

Adopting the generator reference-arrow system, current and power delivered by the battery are positive, i.e., in V2G mode and if the battery is charging, those quantities are negative (G2V mode).

3.2. Control of the Voltage Source Inverter

The control scheme of the VSI is shown in Figure 3 (d) and it is based on the Voltage Oriented Control (VOC) applied to three-phase systems. Three-phase quantities such as grid voltages and currents can be represented by their space phasors which are vectors with two components described in a fixed orthogonal $\alpha\beta$ system. In single-phase systems, the use of such representation is not possible unless a virtual orthogonal component is coupled to the real axis in order to emulate a two axis reference frame. For this purpose, an additional orthogonal component was proposed in (Zhang, *et al.*, 2002) by introducing the imaginary orthogonal circuit concept. Thus, auxiliary orthogonal components are obtained by applying a 90º phase shift with respect to their counterparts in the real circuit. Hence, voltages and currents can be represented by their space phasors:

$$\begin{cases} \bar{v}_{\alpha\beta} = v_\alpha + jv_\beta \\ \bar{i}_{\alpha\beta} = i_\alpha + ji_\beta \end{cases} \tag{1}$$

From the output *LC* filter of Figure 3 (d), and applying Kirchhoff's voltage law,

$$\bar{v}_{c,\alpha\beta} = \bar{v}_{g,\alpha\beta} + R\bar{i}_{\alpha\beta} + Ld\bar{i}_{\alpha\beta}/dt \tag{2}$$

where *R* and *L* are the parasitic resistance and the inductance of the filter, respectively.

The resulting $\alpha\beta$ components are 90º phase shifted sinusoidal signals that can be used for the control of the VSI using classical PI controllers. However, two well-known drawbacks appear: the inability of PI controllers to track sinusoidal references without steady-state error and poor disturbance rejection capability (Teodorescu, *et al.*, 2011). This occurs due to the poor performance of the integral action if the disturbance is a periodic signal. To overcome these drawbacks of PI controllers with a sinusoidal reference and harmonic disturbances, the power control of the VSI can be implemented in a *dq* reference frame rotating at an angular speed $\omega = 2\pi f$, where f is the grid frequency. In this so-called synchronous reference frame, the orthogonal components of the grid voltage and current space phasors are DC quantities and, therefore, classical PI controllers can be used since they achieve zero steady state error at the fundamental frequency and improve their dynamic response.

VOC is based on the use of this synchronous reference frame with the *dq* axes rotating at ω speed and oriented such that the *d* axis is aligned with the grid voltage phasor as drawn in Figure 3 (c). By doing this, the quadrature component of the grid voltage will be zero and, consequently, active and reactive powers can be controlled separately by controlling, respectively, the *d* and *q* components of the grid current as presented hereinafter.

Considering the rotating transformation of a general variable $\bar{x}$, given by $\bar{x}_{\alpha\beta} = \bar{x}_{dq}e^{j\theta} = \bar{x}_{dq}e^{j\omega t}$, where $\theta = \omega t$ is the angle of the rotating reference frame with respect to the fixed $\alpha\beta$ axes, and replacing (1) into (2), after simple mathematical manipulations the following equations are obtained:

$$\begin{cases} v_{c,d} = Ri_d + Ldi_d/dt - \omega Li_q + v_{g,d} \\ v_{c,q} = Ri_q + Ldi_q/dt - \omega Li_d + v_{g,q} \end{cases} \tag{3}$$

From Figure 3 (c) and aligning the *d* axis with the grid voltage phasor results that $v_{g,q}=0$, from which (3) becomes

$$\begin{cases} v_{c,d}=v'_d-\omega L i_q+v_{g,d} \\ v_{c,q}=v'_d-\omega L i_d \end{cases} \tag{4}$$

where

$$\begin{cases} v'_d=Ri_d+L\,di_d/dt \\ v'_q=Ri_q+L\,di_q/dt \end{cases} \tag{5}$$

In the VOC scheme depicted in Figure 3 (d), the reference grid current is composed by two terms: i_d^* and i_q^*. The first one is used to perform the DC-link voltage control and the second one is used to control the reactive power in an independent way. Typically, i_q^* is managed to obtain unity power factor, though the implemented VOC is prepared for reactive power support to the grid, described as follows.

The power control of the grid VSI is based on the instantaneous power theory (Czarnecki, 2006), where the power can be defined in the synchronous reference frame. Assuming that the *d* axis is perfectly aligned with the grid voltage phasor, *i.e.*, $v_{g,q}=0$, therefore, active power and reactive power, in single-phase systems, are proportional to i_d and i_q, respectively, as follows (Samerchur, *et al.*, 2011):

$$\begin{cases} p=1/2\left(v_{g,d}i_d+v_{g,q}i_q\right)=1/2\,v_{g,d}i_d \\ q=1/2\left(v_{g,q}i_d-v_{g,d}i_q\right)=-1/2\,v_{g,d}i_q \end{cases} \tag{6}$$

From the above equation the dq components of the reference current are defined by the active and reactive power reference values:

$$\begin{cases} i_d^*=2P^*/v_{g,d}=2P^*/|v| \\ i_q^*=2Q^*/v_{g,d}=2Q^*/|v| \end{cases} \tag{7}$$

Concerning the active power control, instead of using (7), the i_d^* component of the grid reference current is given by the PI controller in order to maintain the voltage at DC-link constant. The active power control is performed by the boost converter and the reference value is given by the power to be extracted from the battery, in the V2G operation mode, or by the battery charge control algorithm in G2V mode, as depicted in Figure 3 (b).

Finally, the VOC scheme of Figure 3 (d) shows the 90º phase delay block (0,25T - a quarter of the grid period) that creates the virtual quadrature component, allowing the emulation of a two-phase system, and also a PLL block that has been implemented to obtain the angle, θ, of the grid voltage, for reference frame transformation and synchronization purposes. The implemented PLL is a second order generalized integrator (Ciobotaru, 2006).

4. SIMULATION RESULTS

The above mentioned power structure and control strategy have been simulated in order to evaluate the control performance of the bidirectional converter for V2G/G2V integration. The simulation validation was performed using MATLAB/Simulink with simulation time of 2e-6 s and sampling frequency of 10 kHz. The control is carried out with a period of 0,1 ms (1/10 kHz).

In the simulated scenario, with an elapsed time of 4 s, the battery is charging during the first 1,5 s (G2V mode) and in the remaining time interval, it is discharging (V2G mode). At $t=2{,}5$ s the active power reference

changes from 1000 W to 0 W. Then, at $t = 3$ s, the reactive power reference changes from 0 var to -400 var and at $t = 3{,}5$ s it changes from -400 var to +400 var. The simulation results are depicted hereinbelow.

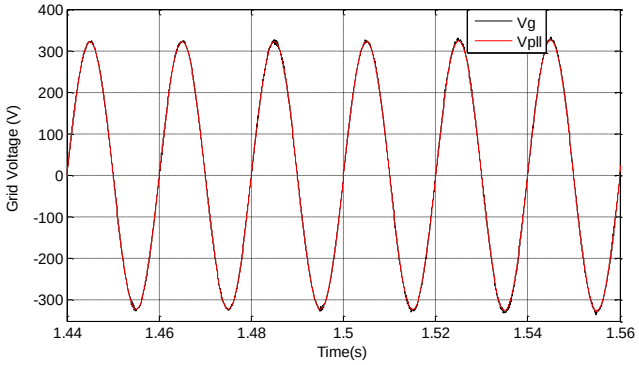

Figure 4.- Grid voltage and PLL output voltage.

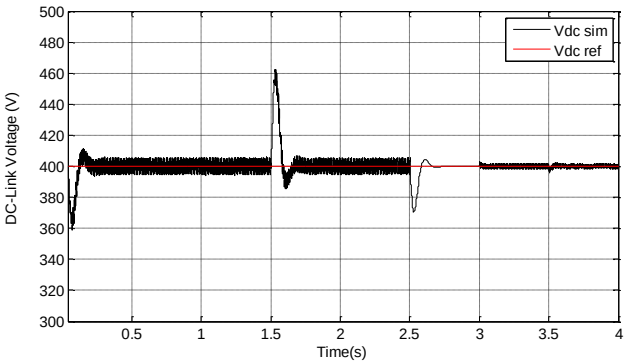

Figure 5.- DC-Link voltage (voltage across the DC-Link capacitor).

The simulated grid voltage, together with the PLL output and the voltage across the DC link capacitor are shown in Figures 4 and 5, respectively. As can be seen from the first one, the PLL fits perfectly the fundamental component of the grid voltage. Regarding the voltage across the DC link capacitor, C_{dc}, (Figure 5) it is composed of a DC component and a pulsating component with double main grid frequency (Rodriguez, *et al.*, 2005). The initial voltage of the capacitor is 400 V and, after an initial transient, the voltage PI controller brings the DC voltage to the reference value. When the power converter changes from G2V to V2G operation mode, then the DC/DC converter changes from "buck" to "boost" operation mode. Consequently, the current changes from about -10 A to 10 A and, therefore, the DC voltage tends to increase dramatically and, consequently, the voltage PI controller rapidly brings the DC voltage to the reference value. At $t = 2{,}5$ s, when the active power reference value is set to zero, no current is sent from the battery to the capacitor and, therefore, the DC voltage tends to decrease but the voltage PI controller brings the DC voltage to the reference value once again. It should be noted that the changes in the reactive power do not affect too much the voltage across the DC-Link capacitor.

Figure 6 shows the voltage and current of the battery during the simulation time span. In G2V mode (during the first 1,5 s), the current reference value is set by the charging algorithm which is -10 A. In V2G mode, it is defined by the power to be extracted from the battery which was set to 1000 W, giving a reference current of about 10 A with a battery voltage of 99,5 V. After the first 2,5 s no power is injected into the grid because the active power reference value is set to zero. Concerning the initial state of charge (SoC) of the battery, it is assumed to be equal to 90%.

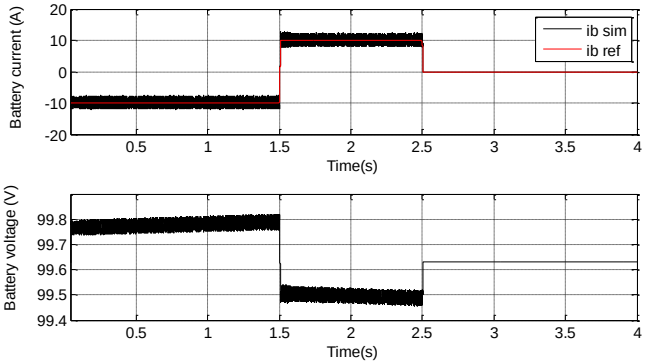

Figure 6.- Battery current (above) and voltage (below).

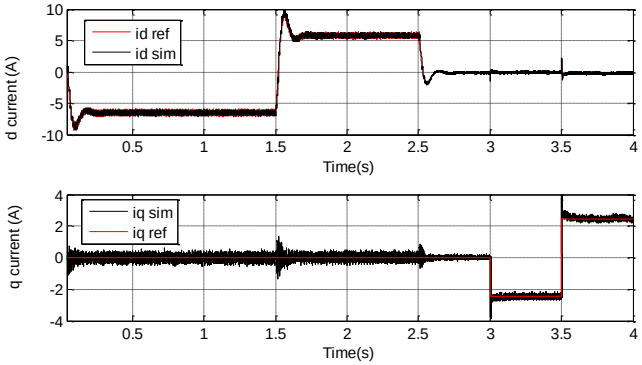

Figure 7.- Grid current components in synchronous reference frame: *d* component (above) and *q* component (below).

The grid current dq components in the synchronous reference frame are depicted in Figure 7. It can be observed that the *d* component, which controls the active power, is negative in G2V operation, positive in V2G mode and zero when the active power reference value is set to zero. On the other hand, the *q* component, which

controls the reactive power, is zero during the first 3 s and then it follows continuously the reactive power changes, that is, from 0 var to -400 var, at 3 s, and from -400 var to +400 var, at $t = 3{,}5$ s.

Figure 8 presents the main details of the instantaneous grid voltage and current as well as the grid current magnitude for different events of the simulation scenario. Figure 8 (a) shows the transition from G2V to V2G mode of operation. As it can be seen, before reaching 1,5 s, the current is in phase opposition with respect to the voltage and after 1,5 s it is in phase. Thus, firstly the power flows from the grid to the battery (negative power) and afterwards from the battery to the grid (positive power). The change from G2V to V2G do not happens at exactly 1,5 s because there is a ramp limiter to avoid a sudden change in the current reference value. The pulsating component of the grid current, which can be seen in the amplitude signal of Figure 8 (a) and (b), is a consequence of the pulsating component of the voltage across the DC-Link capacitor, which is due to the grid frequency, as previously mentioned (Khajehoddin, *et al.*, 2008).

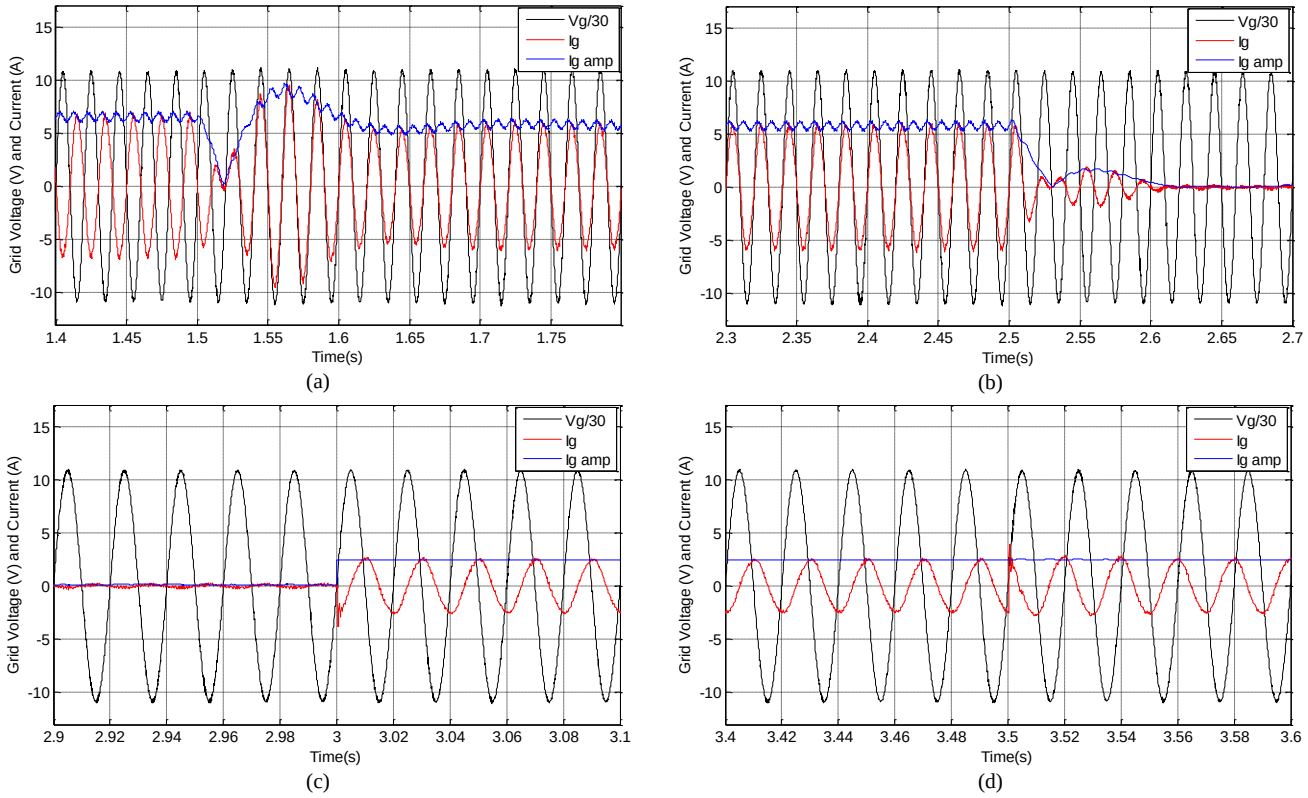

Figure 8.- Grid voltage (scaled) and grid current (the red and blue lines are the instantaneous current and its magnitude, respectively) during (a) the change from G2V to V2G mode of operation (at $t = 1{,}5$ s), (b) the change in the active power reference from 1000 W to 0 W (at $t = 2{,}5$ s), (c) the change in the reactive power reference from 0 var to -400 var (at $t = 3$ s) and (d) the change in the reactive power reference from -400 var to +400 var (at $t = 3{,}5$ s).

At $t = 2{,}5$ s the active power reference changes from 1000 W to 0 W and, after a transient, the current reduces to zero, as can be seen in Figure 8 (b). This event was simulated in order to validate the control of the reactive power by the inverter upon a lagging and leading grid power factor. Thus, at $t = 3$ s, a step of -400 var is set in the reactive power reference and, therefore, the grid current lags the voltage by 90º, as can be seen in Figure 8 (c). This means that the VSI is absorbing reactive power from the grid. Therefore, at this time instant, the q component of the grid current, in the synchronous reference frame, changes from 0 to a negative value (about -2,4 A), as observed in Figure 7. At $t = 3{,}5$ s, and keeping the active power set to zero, the reference of the reactive power is changed from -400 var to +400 var, meaning that that the VSI is now delivering reactive power to the grid. At this time instant, the q component of the grid current, in the synchronous reference frame, changes from -2,4 A to 2,4 A, as can be observed in Figure 7. These current values are the ones required to absorb a specified inductive reactive power and to deliver a capacitive reactive power, respectively.

The evolution of *d* component of the grid current during the simulation time interval is shown in Figure 7. As expected, the *d* component of the grid current does not vary with the changes in the reactive power but the rms value of the grid current increases when a step of -400 var is applied, as can be seen in Figure 8 (c). Obviously, the rms value is the same when the reactive power changes from -400 var to +400 var, but the current stops lagging the voltage and starts leading the grid voltage by an angle of 90º, as shown in Figure 8 (d).

5. CONCLUSIONS

This paper presented an on-going implementation and validation, throughout simulation, of a power converter topology for a V2G/G2V interface, for the integration of a light electric vehicle, with a lithium ion phosphate battery, under a 5 kW microgrid project. Simulation results showed that the adopted topology and control strategy is able to manage bidirectional active and reactive power flow allowing power factor compensation and, on the other hand, the battery behaves as an electric load or generator and improves the storage capability of the microgrid. By this way, the vehicle battery and its interface may collaborate to the reliability and quality criteria of the energy supply.

REFERENCES

Ciobotaru, M.; Teodorescu, R.; Blaabjerg, F.; (2006). A New Single-Phase PLL Structure Based on Second Order Generalized Integrator. In 37th *IEEE Power Electronics Specialists Conference (PESC '06)*. 18-22 June, 2006. pp. 1-6.

Czarnecki, L. S. (2006). Instantaneous Reactive Power p-q Theory and Power Properties of Three-Phase Systems. *IEEE Transactions on Power Delivery*. Vol. 21 (January 2006). pp. 362-367.

EVI; IEA; (2013). Global EV outlook. Understanding the Electric Vehicle Landscape to 2020. Electric Vehicles Initiative (EVI) and International Energy Agency (IEA). Available from: http://www.iea.org/

Ferdowsi, M.; (2007). Plug-in Hybrid Vehicles - A Vision for the Future. In *IEEE Vehicle Power and Propulsion Conference (VPPC 2007)*. Arlington, Texas, 9-12 September, 2007.

Guerrero, J. M., *et al.*; (2013b). Advanced Control Architectures for Intelligent Microgrids—Part II: Power Quality, Energy Storage, and AC/DC Microgrids. *IEEE Transactions on Industrial Electronics*. Vol. 60, n.º 4 (April, 2013). pp. 1263 – 1270.

Guerrero, J. M. , *et al.*; (2013a). Advanced Control Architectures for Intelligent Microgrids—Part I: Decentralized and Hierarchical Control. *IEEE Transactions on Industrial Electronics*. Vol. 60, n.º 4 (April, 2013). pp. 1254 – 1262.

Hua, A. C.-C.; Syue, B. Z.-W.; (2010). Charge and Discharge Characteristics of Lead-Acid Battery and LiFePO4 Battery. In *International Power Electronics Conference (IPEC 2010)*. 21-24 June 2010. pp. 1478-1483.

IEA; (2012). *World Energy Outlook*. Technical report. Paris, France, International Energy Agency Publications.

Khajehoddin, S.A., *et al*.; (2008). A robust power decoupler and maximum power point tracker topology for a grid-connected photovoltaic system. In *Power Electronics Specialists Conference (PESC 08)*. June, 2008. pp. 66–69.

Leite, V., *et a*l.; (2014). Bidirectional Vehicle-to-Grid Interface under a Microgrid Project. In *15th IEEE Workshop on Control and Modeling for Power Electronics (COMPEL 2014)*. Santander, Spain, June 22-25, 2014.

Leite, V., *et al*.; (2013a). On the Implementation of a Microgrid Project with Renewable Distributed Generation. In *I Congreso Iberoamericano sobre Microrredes con Generación Distribuida de Renovables*. Soria, Spain, 23-24 September, 2013.

Leite, V., *et al*.; (2013b). The IPB ECO Buggy – A Light Electric Vehicle in a Live Park of Renewable Energies. In *17th International Symposium Power Electronics (Ee2013)* Novi Sad, Republic of Serbia, 30 October-1 November, 2013.

Leite, V.; Batista, J.; Rodrigues, O.; (2012a). VER*Campus* – Live Park of Renewable Energies. In *International Conference on Renewable Energies and Power Quality, (ICREPQ'12)*. Santiago de Compostela, Spain, 28-30 March, 2012.

Leite, V., *et al*.; (2012b). Dealing with the Very Small: First Steps of a Picohydro Demonstration Project in an University Campus. In *International Conference on Renewable Energies and Power Quality (ICREPQ'12)*. Santiago de Compostela, Spain, 28-30 March, 2012.

Olivier, J. G., *et al*.; (2013). *Trends in global CO_2 Emissions: 2013 Report*. PBL Netherlands Environmental Assessment Agency and IES of the European Comissions's Joint Research Centre (JRC). The Hague. Netherlands. PBL Publishers.

Rodriguez, J.R., *et al*.; (2005). PWM regenerative rectifiers: state of the art. *IEEE Transactions on Industrial Electronics*. Vol. 52, n.º 1 (Feb. 2005). pp. 5-22.

Saber, A. Y.; Venayagamoorthy, G. K.; (2009). One Million Plug-in Electric Vehicles on the Road by 2015. In *12th International IEEE Conference on Intelligent Transportation Systems (ITSC '09)*. St. Louis, MO, 4-7 October, 2009. pp. 1-7.

Saber, A. Y.; Venayagamoorthy, G. K.; (2011). Plug-in Vehicles and Renewable Energy Sources for Cost and Emission Reductions. *IEEE Transactions on Industrial Electronics*. Vol. 58, n.º 4 (April, 2011). pp. 1229-1238.

Samerchur, S., *et al*.; (2011). Power Control of Single-Phase Voltage Source Inverter for Grid-Connected Photovoltaic Systems. In *Power Systems Conference and Exposition (PSCE), IEEE/PES*. 20-23 March, 2011. pp. 1-6.

Teodorescu, R., et al.; (2011). *Grid Converters for Photovoltaic and Wind Power Systems*. John Wiley & Sons.

Tingting, D., *et al*.; (2011). Analysis on the Influence of Measurement Error on State of Charge Estimation of LiFePO4 Power Battery. In *International Conference on Materials for Renewable Energy & Environment (ICMREE 2011)*. Shanghai, 20-22 May, 2011. Vol.1, pp. 644-649.

UNEP; (2013). Renewable 2013. Global Status Report. REN21 Secretariat. Paris. Available from: http://www.ren21.net/

Yilmaz, M.; Krein, P. T.; (2013). Review of the Impact of Vehicle-to-Grid Technologies on Distribution Systems and Utility Interfaces. *IEEE Transactions on Power Electronics*. Vol. 28. pp. 5673-5689.

Zandi, M., *et al*.; (2011). Energy Management of a Fuel Cell/Supercapacitor/Battery Power Source for Electric Vehicular Applications. *IEEE Transactions on Vehicular Technology*. Vol. 60. pp. 433-443.

Zhang, F.; Cooke, P.; (2010). *The Green Vehicle Trend: Electric, Plug-in hybrid or Hydrogen fuel cell?*. Dynamics of Institutions and Markets in Europe (DIME). Available from: http://www.dime-eu.org/

Zaghib, K., *et al*.; (2004). LiFePO4/polymer/natural graphite: low cost Li-ion batteries. *Electrochimica Acta, ELSEVIER*. Vol. 50, n.º 2–3. pp. 263-270.

Zhang, R., *et al*.; (2002). A grid Simulator with Control of Single-Phase Power Converters in D-Q Rotating Frame. In *IEEE 33rd Annual Power Electronics Specialists Conference (PESC 02)*. 23-27 June, 2002. pp. 1431-1436.